S4-43
005152
317465

# GEOCODING OF AIRSAR/TOPSAR SAR DATA


Francesco Holecz *, Yunling Lou, and Jakob van Zyl

Jet Propulsion Laboratory
California Institute of Technology
4800 Oak Grove Drive, M/S 300-243
Pasadena, CA 91109
E-mail: franci@blacks.jpl.nasa.gov
FAX: +1 818 354 0495

* on leave from Remote Sensing Laboratories, University of Zürich, Switzerland


## 1. INTRODUCTION

It has been demonstrated and recognized that radar interferometry is a promising method for the determination of digital elevation information (Zebker et al., 1994; Madsen et al., 1995) and terrain slope (Wegmüller et al., 1993) from Synthetic Aperture Radar (SAR) data. An important application of Interferometric SAR (InSAR) data in areas with topographic variations is that the derived elevation and slope can be directly used for the absolute radiometric calibration of the amplitude SAR data (van Zyl et al., 1993; Holecz et al., 1994), as well as for scattering mechanisms analysis (van Zyl, 1993; Holecz et al., 1995). On the other hand polarimetric SAR data has long been recognized as permitting a more complete inference of natural surfaces than a single channel radar system. In fact, imaging polarimetry provides the measurement of the amplitude and relative phase of all transmit and receive polarizations.

On board the NASA DC-8 aircraft, NASA/JPL operates the multifrequency (P, L and C bands) multipolarimetric radar AIRSAR (van Zyl et al., 1992). The TOPSAR, a special mode of the AIRSAR system, is able to collect single-pass interferometric C- and/or L-band VV polarized data (van Zyl et al., 1995). A possible configuration of the AIRSAR/TOPSAR system is to acquire single-pass interferometric data at C-band VV polarization and polarimetric radar data at the two other lower frequencies. The advantage of this system configuration is to get digital topography information at the same time the radar data is collected. The digital elevation information can therefore be used to correctly calibrate the SAR data. This step is directly included in the new AIRSAR Integrated Processor. This processor uses a modification of the full motion compensation algorithm described by Madsen et al. (1993). However, the Digital Elevation Model (DEM) with the additional products such as local incidence angle map, and the SAR data are in a geometry which is not convenient, since especially DEMs must be referred to a specific cartographic reference system. Furthermore, geocoding of SAR data is important for multisensor and/or multitemporal purposes. In this paper, a procedure to geocode the new AIRSAR/TOPSAR data is presented. As an example an AIRSAR/TOPSAR image acquired in 1994 is geocoded and evaluated in terms of geometric accuracy.

## 2. THE AIRSAR INTEGRATED PROCESSOR

A complete description of the AIRSAR/TOPSAR products is given in van Zyl (1995). Here we briefly present the different output data types. The Integrated AIRSAR Processor produces two data products: the standard AIRSAR products in frame and synoptic format, and the integrated TOPSAR product. The last one consists of a number of different data types, namely:

- **Digital Elevation Model** , which represents the elevation of the terrain above a spherical approximation to the World Geodetic System 84 (WGS84). The data are stored as two bytes.
- **C-band VV polarized** calibrated amplitude data as acquired with the top antenna in the TOPSAR mode. The radiometric corrections are performed taking into account the topography when removing the antenna patterns and the scattering areas. The data are stored as two bytes.
- **Local incidence angle map** derived using the digital elevation model information. The data are stored as one byte.
- **Correlation map** contains the normalized correlation coefficient between the two C-band interferometric channels. The data are stored as one byte.
- **L-band polarimetry data** contain the calibrated AIRSAR compressed Stokes matrix data at L-band. Each pixel is represented by ten bytes.
- **P-band polarimetry data** contain the calibrated AIRSAR compressed Stokes matrix data at P-band. Each pixel is represented by ten bytes.

The selected radar mapping coordinate system $(s, c, h_r)$ is defined relative to the sphere tangent to the WGS84 ellipsoid at longitude $\lambda_p$ and latitude $\varphi_p$ - referred to as the peg point and approximately corresponding to the center of the image - having a radius $r_a$, which is the radius of curvature in the along track direction (Hensley, 1993). In this system, $s$ and $c$ are distances in along and across direction, while $h_r$ is the height above the approximating sphere.

## 3. FROM THE RADAR MAPPING TO MAP COORDINATE SYSTEM

This section describes the transformation from the radar mapping coordinates $(s, c, h_r)$ into the map coordinates $(x, y, h_o)$. An accurate transformation of the derived DEM data into map coordinates is only possible by using a forward transform. In fact, by applying a backward transform, which has the advantage of fewer number of calculations, the pixel location in the map coordinate system can be inaccurate, because the pixel altitude $h_o$ is usually unknown. Thus, the following geodetic and cartographic transformation steps must be carried out:

1. From radar mapping $(s, c, h_r)$ into global Cartesian coordinates $(X, Y, Z)$
2. From global Cartesian into local Cartesian coordinates $(X', Y', Z')$
3. From local Cartesian into geographic coordinates $(\lambda, \varphi, h_e)$
4. From geographic into map coordinates $(x, y, h_o)$

A forward transform implies that the output product can contain holes, if inappropriately implemented. To avoid gaps in the output data, four map coordinates, corresponding to four DEM corners in the radar mapping coordinates, define the orientation and the surface of the pixel. The area is then filled using a polygon fill algorithm. This procedure is subsequently applied to each pixel of the input data. In order to be computationally efficient, the transformation of radar coordinate positions for each pixel to the map coordinate system is stored in a two dimensional look-up table. Thus, all additional input products, such as local incidence angle map, correlation map, and SAR data can be very easily and efficiently geocoded using the same look-up table.

The first step is to transform the DEM data from the radar coordinates into the global Cartesian coordinates (in this case the WGS84 system), namely:

$$\begin{pmatrix} X \\ Y \\ Z \end{pmatrix} = \mathbf{M_1 M_2} \begin{pmatrix} (r_a + h_r)\cos c_\varphi \cos s_\lambda \\ (r_a + h_r)\cos c_\varphi \sin s_\lambda \\ (r_a + h_r)\sin c_\varphi \end{pmatrix} + \mathbf{O}$$

where

$$\mathbf{M_1} = \begin{pmatrix} -\sin\lambda_p & -\sin\varphi_p\cos\lambda_p & \cos\varphi_p\cos\lambda_p \\ \cos\lambda_p & -\sin\varphi_p\sin\lambda_p & \cos\varphi_p\sin\lambda_p \\ 0 & \cos\varphi_p & \sin\varphi_p \end{pmatrix}$$

$$\mathbf{M_2} = \begin{pmatrix} 0 & \sin\eta & -\cos\eta \\ 0 & \cos\eta & \sin\eta \\ 1 & 0 & 0 \end{pmatrix}$$

$$\mathbf{O} = \begin{pmatrix} r_e(\varphi_p)\cos\varphi_p\cos\lambda_p \\ r_e(\varphi_p)\cos\varphi_p\sin\lambda_p \\ r_e(\varphi_p)(1-e^2)\sin\varphi_p \end{pmatrix} - \begin{pmatrix} r_a\cos\varphi_p\cos\lambda_p \\ r_a\cos\varphi_p\sin\lambda_p \\ r_a\sin\varphi_p \end{pmatrix}$$

$$r_a = \frac{r_e(\varphi_p)r_n(\varphi_p)}{r_e(\varphi_p)\cos^2\eta + r_n(\varphi_p)\sin^2\eta}$$

$$r_e(\varphi_p) = \frac{a}{(1-e^2\sin\varphi_p)^{\frac{1}{2}}}$$

$$r_n(\varphi_p) = \frac{a(1-e^2)}{(1-e^2\sin\varphi_p)^{\frac{3}{2}}}$$

$r_e$ and $r_n$ are the East and North radius of curvature at the peg point, $\eta$ is the heading (or track angle), $c_\varphi = c/r_a$, $s_\lambda = s/r_a$, $\mathbf{O}$ is a translation vector, $\mathbf{M_1}$ and $\mathbf{M_2}$ are transformation matrices, $a$ and $e^2$ are the semi-major axis and the ellipticity of the WGS84 ellipsoid ($a$ = 6378137 m, $e^2 = 0.00669437999015$). Basically, to specify the transformation from the radar mapping coordinates to the Earth centered Cartesian coordinate system, only three parameters are required, namely the latitude and longitude of the peg point, and the heading of the reference curve at the peg point.

Since the ellipsoid origin of a given cartographic reference system is not necessarily coincident with the Earth center and their shape and size may vary considerably, geodetic datums must be considered. The datum transformation is described by the three dimensional Helmert transformation (Frei et al., 1993), namely:

$$\begin{pmatrix} X \\ Y \\ Z \end{pmatrix} = \begin{pmatrix} \Delta x \\ \Delta y \\ \Delta z \end{pmatrix} + (1+m)\mathbf{D} \begin{pmatrix} X' \\ Y' \\ Z' \end{pmatrix}$$

where

$$\mathbf{D} = \begin{pmatrix} \cos\beta\cos\gamma & \cos\alpha\sin\gamma + \sin\alpha\sin\beta\sin\gamma & \sin\alpha\sin\gamma - \cos\alpha\sin\beta\cos\gamma \\ -\cos\beta\sin\gamma & \cos\alpha\cos\gamma - \sin\alpha\sin\beta\sin\gamma & \sin\alpha\cos\gamma + \cos\alpha\sin\beta\sin\gamma \\ \sin\beta & -\sin\alpha\cos\beta & \cos\alpha\cos\beta \end{pmatrix}$$

and $(\Delta x, \Delta y, \Delta z)$ are translation parameters, $m$ a scaling parameter, and $(\alpha, \beta, \gamma)$ three rotation parameters.

Now, the transformation from the local Cartesian coordinates into the geographic coordinates can be carried out, namely:

$$\varphi = \arctan \frac{Z' + (e')^2 b \sin^3\theta}{d - e^2 a \cos^3\theta}$$

$$\lambda = \frac{Y'}{X'}$$

$$h_e = \frac{d}{\cos\varphi} - \nu$$

where

$$e^2 = \frac{a^2 - b^2}{a^2}$$

$$(e')^2 = \frac{a^2 - b^2}{b^2}$$

$$\nu = \frac{a}{(1 - e^2\sin^2\varphi)^{\frac{1}{2}}}$$

$$d = [(X')^2 + (Y')^2]^{\frac{1}{2}}$$

$$\theta = \arctan \frac{Z'a}{db}$$

Note that $a$ and $b$ are the semi-major and semi-minor axes of the ellipsoid used in a given country. Furthermore, not all countries provide the solution of the 7 parameters (i.e. $\Delta x, \Delta y, \Delta z, m, \alpha, \beta, \gamma$). In those cases, usually, only the three translation parameters must be known.

The last step is to transform the geographic coordinates into a desired map coordinate system. The much used projections are the Universal Transfer Mercator, the Oblique Mercator, the Lambert Conformal Conic Projection, and the Stereographic Projection. A detailed description is given in Snyder (1987). As an example, we consider here the UTM system:

$$x = x_o + k_1\Delta\lambda + k_3\Delta\lambda^3 + k_5\Delta\lambda^5$$

$$y = y_o + k_0 + k_2\Delta\lambda^2 + k_4\Delta\lambda^4 + k_6\Delta\lambda^6$$

where $x_o$ and $y_o$ are the false origin coordinates, $\Delta\lambda = (\lambda - \lambda_o)$ with $\lambda_o$ the geographic longitude of the central meridian, and $k_0 ... k_6$ are coefficients (see Snyder, 1987). Note, $x$ refers to the Easting coordinates, while $y$ to the Northing coordinates. It should be noted that to obtain orthometric heights $h_o$, ellipsoidal heights $h_e$ need to be corrected for the geoidal heights $h_g$ according to $h_o \cong h_e - h_g$.

## 4. RESULTS

The SAR data used in this study were collected by the NASA/JPL AIRSAR/TOPSAR system in 40 MHz mode on April 12, 1994 over the area of Atlanta airport (33.76°N, 83.59°W), Georgia. The data have a postprocessing pixel spacing of 10 meters and cover an area of around 100 km$^2$. The DEM was geocoded to the UTM coordinate system zone 16 (central meridian 87°) taking into account the North American Datum 1927 (Clarke ellipsoid 1866, $\Delta x$ = -9 m with $\sigma_{\Delta x}$ = 5 m, $\Delta y$ = 161 m with $\sigma_{\Delta y}$ = 5 m, $\Delta z$ = 179 m with $\sigma_{\Delta z}$ = 8 m).

Figure 1 represents the location accuracy for 8 selected ground control points without using (left) and by using some independent ground control points (right). Figure 2 shows the geocoded DEM (a) with the corresponding correlation map (b), the derived local incidence angle map (c), the C-band VV-polarized amplitude data (d), the L-band HH-polarized amplitude data (e), and the L-band HV-polarized amplitude data (f).

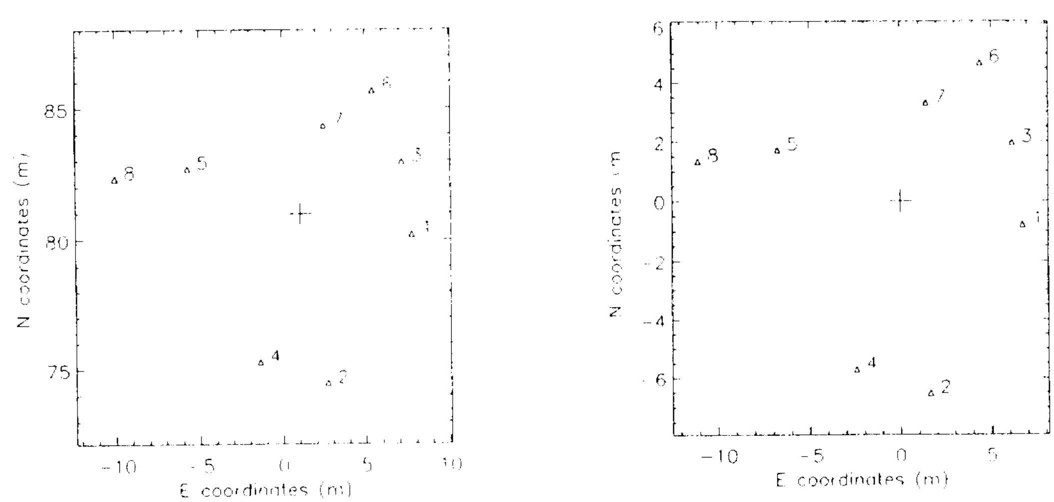


Figure 1: Positioning accuracy without (left) and with ground control points (right).

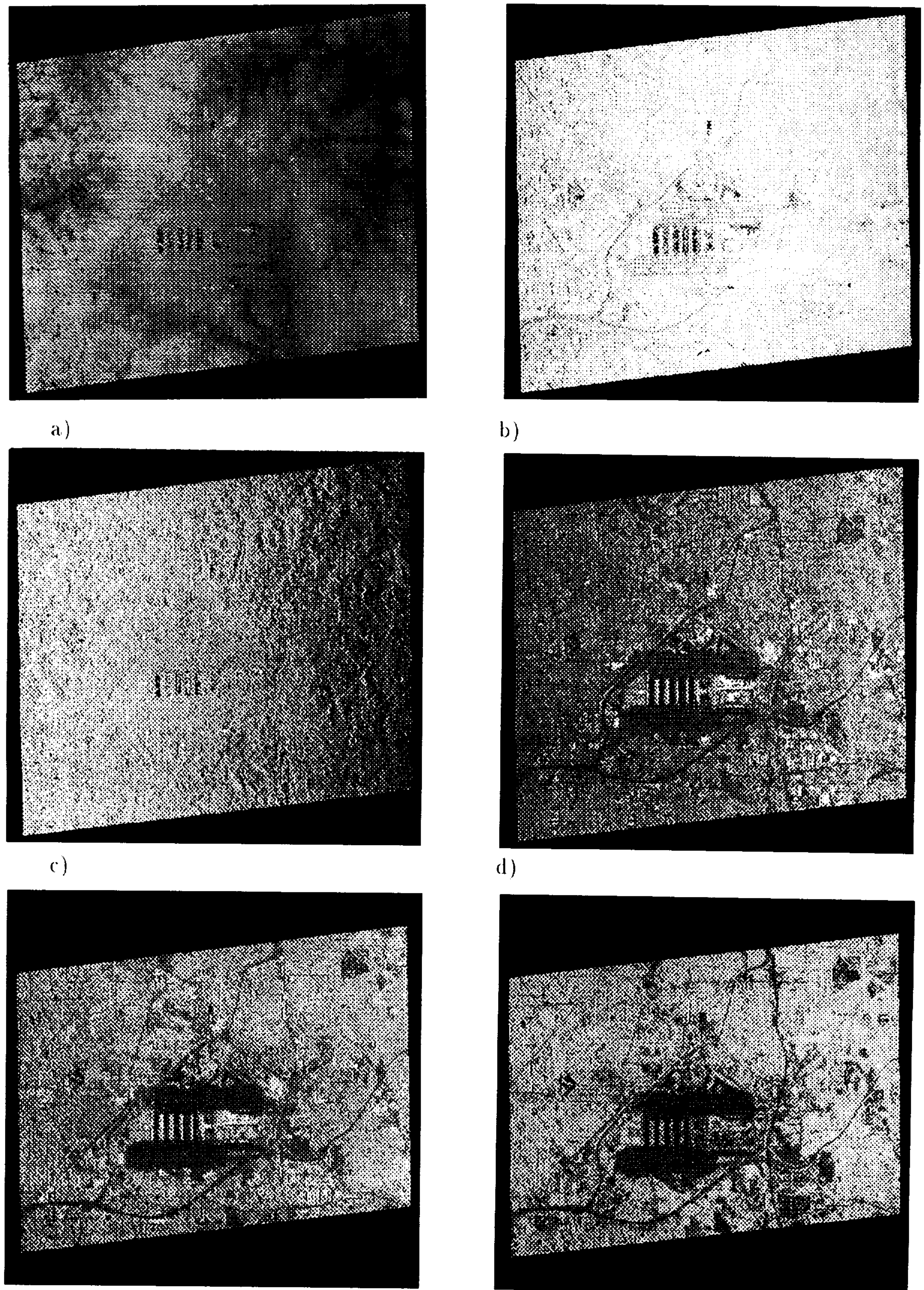


Figure 2: Geocoded AIRSAR/TOPSAR products in UTM zone 16 a) DEM, b) Correlation map, c) Local incidence angle map, d) C-VV data, e) L-HH data, f) L-HV data.

An important prerequisite for accurate geocoding is precise flight path data. Currently, the NASA DC-8 aircraft is equipped with the Honeywell H-764G Inertial Navigation System (INS) with an embedded Global Positioning System (GPS) receiver. This system, which has an acquisition rate of 50 Hz, meets a position accuracy of $\leq 16$ meters, a pitch and roll accuracy of $\leq 0.01$ degrees, and a heading accuracy of $\leq 0.02$ degrees (Honeywell, 1993). Note that this GPS performance is obtained during a period of normal GPS coverage with a Position Dilution of Precision of 3.2 or less, and P(Y)-Code receiver mode. In other words, using this flight path data accuracy, and also considering the uncertainties of the datums' shift parameters, a geocoding precision of $\pm 1$ pixel is expected, assuming a postprocessing pixel spacing of 10 meters.

Figure 1 (left) clearly shows in the $y-$direction, i.e. N-S direction, an average location error of around 80 meters (corresponding to 8 pixels in the DEM data), while in the $x-$direction it is about 1 pixel. However, by using 1 ground control point, these inaccuracies are reduced, resulting in a final positioning precision on the order of $\pm 1$ pixel (Figure 1 right). A possible explanation of the observed error in $y-$direction could be figured in a time synchronization problem between the GPS measurements and the SAR data. In fact, the flight track angle $\eta$ in this case was of $0^{o}$, i.e. S-N direction, and therefore positioning inaccuracies in the $y-$direction were mainly affected. It should be noted that the position of the 8 ground control points was determined by using a 1:24,000 scale map of the U.S. Geological Survey. Therefore, some minor inaccuracies due to the map scale must also be considered.

## 5. CONCLUSIONS

In this paper we presented a procedure to geocode the new AIRSAR/TOPSAR data. Furthermore, it was shown that geocoding of these data is well defined, without using, as is often done, transformations based on polynomials, which can strongly affect the geometric accuracy. Using geodetic and cartographic transforms, the geocoding can basically be carried out without the need of ground control points, which sometimes can be difficult, especially for those areas where the availability of topographic maps is almost impossible. At this time, we are testing this procedure for data sets acquired during the 1994 and 1995 campaigns in order to figure out the above mentioned error. In addition, we are planning to optimize the geocoding procedure without using the intermediary $(s, c, h_r)$ radar mapping system. This will allow a straight geocoding from slant range to a given reference map coordinate system, in order to deliver to the users geocoded AIRSAR/TOPSAR data.

## ACKNOWLEDGMENTS

This study was supported by the Swiss Academy of Science and the Holderbank Foundation. A portion of the research described in this paper was performed by the Jet Propulsion Laboratory, California Institute of Technology, under a contract with the National Aeronautics and Space Administration.

## REFERENCES


Frei U., C. Graf, and E. Meier, 'Cartographic reference systems', Chapter 10 in SAR-Geocoding - Data and Systems, Wichmann-Verlag, Karlsruhe, Germany, edited by G. Schreier, 1993.

Hensley S., 'Interoffice Memorandum 3346-93-163' (internal document), Jet Propulsion Laboratory, Pasadena, Calif., 1993.

Holecz F., E. Meier, J. Piesbergen, D. Nüesch, and J. Moreira, 'Rigorous derivation of the backscattering coefficient', IEEE Geoscience and Remote Sensing Newsletter, No. 92, September, 1994.

Holecz F., U. Wegmüller, E. Rignot, and Y. Wang, 'Observed radar backscatter from forested areas with terrain variations', Proceedings IGARSS'95, Firenze, 1995.

Honeywell, 'Detailed specification for the H-764G Inertial Navigation System (INS) with an embedded Global Positioning System (GPS) receiver', Avionics Division, St. Petersburg, Florida, 1993.

Madsen S., H. Zebker, and J. Martin, 'Topographic mapping using radar interferometry: Processing techniques', IEEE Transactions on Geoscience and Remote Sensing, Vol. 31, No. 1, 1993.

Madsen S., J. Martin, and H. Zebker, 'Analysis and evaluation of the NASA/JPL TOPSAR across-track interferometric SAR system', IEEE Transactions on Geoscience and Remote Sensing, Vol. 33, No. 2, 1995.

Snyder J., 'Map projections used by the U.S. Geological Survey', Geological Survey Bulletin 1532, United States Government Printing Office, Washington DC, 1987.

van Zyl J., R. Carande, Y. Lou, T. Miller, and K. Wheeler, 'The NASA/JPL three frequency polarimetric AIRSAR System', Proceedings IGARSS'92, Houston, 1992.

van Zyl J., 'The effect of topography on radar scattering from vegetated areas', IEEE Transactions on Geoscience and Remote Sensing, Vol. 31, No. 1, 1993.

van Zyl J., B. Chapman, P. Dubois, and J. Shi, 'The effect of topography on SAR calibration', IEEE Transactions on Geoscience and Remote Sensing, Vol. 31, No. 5, 1993.

van Zyl J., 'AIRSAR Integrated Processor Documentation' Version 0.01 (internal document), Jet Propulsion Laboratory, Pasadena, Calif., 1995.

van Zyl J., H. Zebker, S. Hensley, D. Haub, and W. Wiesbeck, 'The new dual frequency (C- and L-band) TOPSAR airborne interferometric SAR', Proceedings IGARSS'95, Firenze, 1995.

Wegmüller U., C. Werner, and P. Rosen, 'Derivation of terrain slope from SAR interferometric phase gradient', Second ERS-1 User Symposium, Hamburg, 1993.

Zebker H., C. Werner, P. Rosen, and S. Hensley, 'Accuracy of topographic maps derived from ERS-1 interferometric radar', IEEE Transactions on Geoscience and Remote Sensing, Vol. 32, No. 4, 1994.